

# 2010 LLNL Nuclear Forensics Summer Program

Glenn T. Seaborg Institute Lawrence  
Livermore National Laboratory Physical  
and Life Sciences  
Livermore, CA 94550, USA

Director: Annie Kersting (kersting1@llnl.gov)  
Education Coordinator: Nancy Hutcheon  
Administrator: Camille Vandermeer Website  
<https://seaborg.llnl.gov>

## **Sponsors:**

National Technical Nuclear Forensics Center, Domestic Nuclear Detection  
Office, Department of Homeland Security  
LLNL: Glenn T. Seaborg Institute, Physical and Life Sciences Directorate



LLNL-AR-450120

The Lawrence Livermore National Laboratory (LLNL) Nuclear Forensics Summer Program is designed to give both undergraduate and graduate students an opportunity to come to LLNL for 8-10 weeks during the summer for a hands-on research experience. Students conduct research under the supervision of a staff scientist, attend a weekly lecture series, interact with other students, and present their work in poster format at the end of the program. Students also have the opportunity to participate in LLNL facility tours (e.g. National Ignition Facility, Center of Accelerator Mass-spectrometry) to gain a better understanding of the multi-disciplinary science that is on-going at LLNL.

Currently called the Nuclear Forensics Summer Program, this program began ten years ago as the Actinide Sciences Summer Program. The program is run within the Glenn T. Seaborg Institute in the Physical and Life Sciences Directorate at LLNL. The goal of Nuclear Forensics Summer Program is to facilitate the training of the next generation of nuclear scientists and engineers to solve critical national security problems in the field of nuclear forensics. We select students who are majoring in physics, chemistry, nuclear engineering, chemical engineering and environmental sciences. Students engage in research projects in the disciplines of actinide and radiochemistry, isotopic analysis, radiation detection, and nuclear engineering in order to strengthen the ‘pipeline’ for future scientific disciplines critical to DHS (DNDO), NNSA.

This is a competitive program with over 200 applicants for the 8-10 slots available. Students come highly recommended from universities all over the country. For example, this year we hosted students from UC Davis, Cal State San Louis Obispo, Univ. of Nevada, Univ. of Wyoming, Northwestern, Univ. of New Mexico and Arizona State Univ (See Table 1). We advertise with mailers and email to physics, engineering, geochemistry and chemistry departments throughout the U.S. We also host students for a day at LLNL who are participating in the D.O.E. sponsored “*Summer School in Nuclear Chemistry*” course held at San Jose State University and have recruited from this program.

This year students conducted research on such diverse topics as: isotopic fingerprinting, statistical modeling in nuclear forensics, uranium analysis for nuclear forensics, environmental radiochemistry, radiation detector materials development, coincidence counting methods, nuclear chemistry, and actinide separations chemistry.

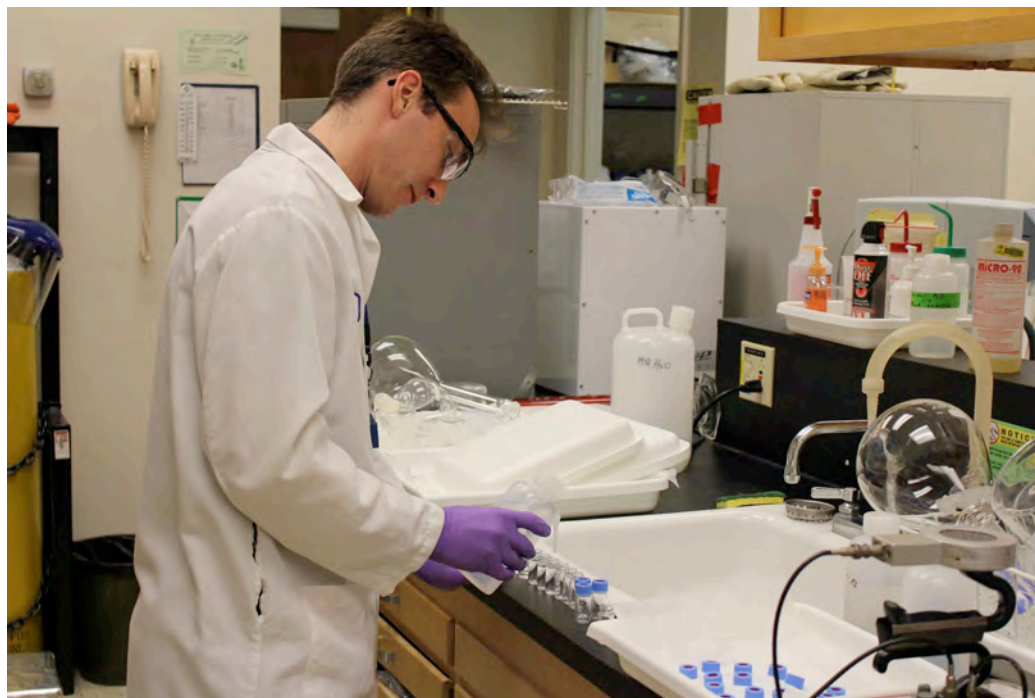
In addition to hands on training, students attend a weekly lecture series on topics applicable to the field of nuclear forensics (see Table 2). Speakers are experts from both within and external to LLNL. Speakers are able to discuss the importance of their work in the context of advances in the field of nuclear forensics.

Graduate students are invited to return for a second year at their mentor’s discretion. For the top graduate students in our program, we encourage the

continuation of research collaboration between graduate student, faculty advisor and laboratory scientists. This creates a successful pipeline of top quality students from universities across the U.S. Since 2002, 29 summer students have continued to conduct their graduate research at LLNL, 9 have become postdoctoral fellows, and 9 have been hired as career scientists. Two summer students have gone on to work at other national laboratories.

A big factor in the success of this program is the dedication of the staff scientists who volunteer to mentor the summer students. In FY10, funding from The Nuclear Forensics Graduate Mentoring Program (sponsor: DNDO) helped to partially support the time staff took to teach the summer interns. Staff scientists could take the necessary time to develop an appropriate summer project, oversee the safety training and dedicate more time helping the interns maximize their productivity.

## 2010 Summer Students at Work





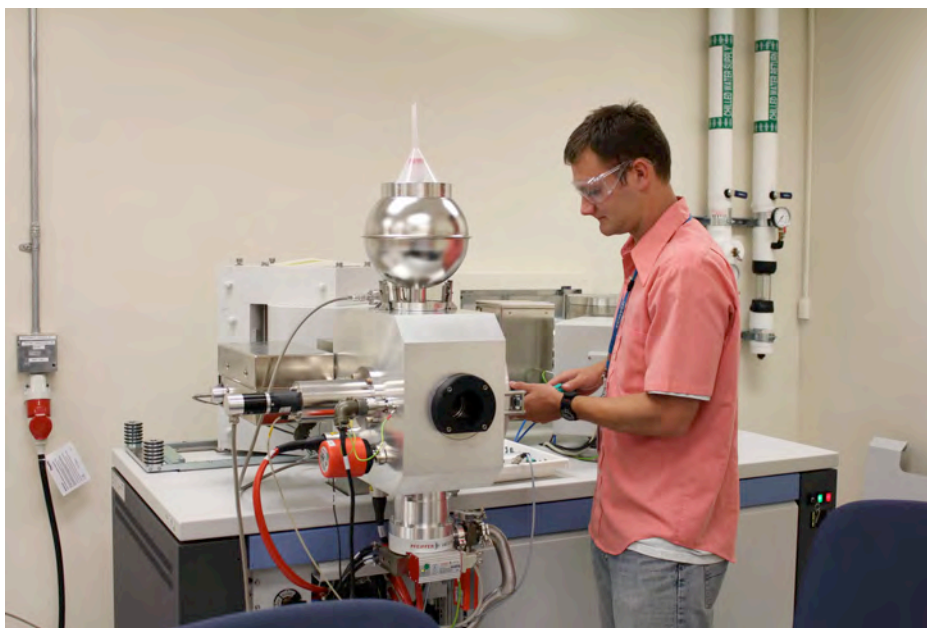
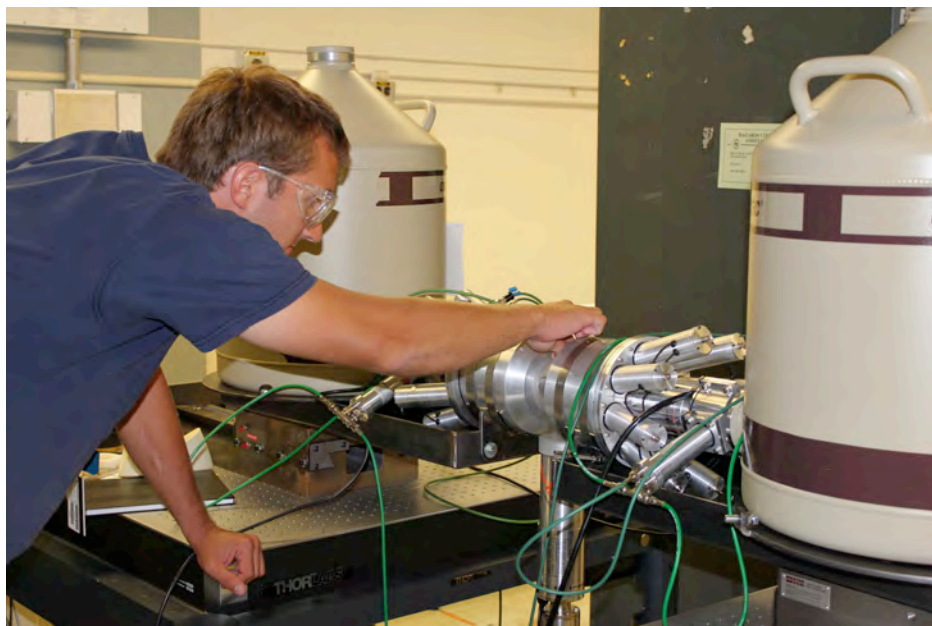


## Table 1 Summer Student Roster 2010

<b><u>Student</u></b>	<b><u>Major</u></b>	<b><u>University</u></b>	<b><u>Year</u></b>
Cameron Bates	Nuc. Engineering	UC Berkeley	Grad
Megan Bennett	Radiochemistry	Univ. Nevada Las Vegas	Grad
Greg Brennecka	Geochemistry	Arizona State Univ.	Grad
Meghali Chopra	Chemistry	Stanford	Undergrad
Eric Dieck	Hydrology	Illinois State University	Grad
Steven Horne	Nuc. Engineering	U Texas	Grad
Marianna Mao	Math/Physics	Harvard	Undergrad
Christopher Matthews	Nuc. Engineer	Oregon State University	Grad
Jon Oiler	Geochemistry	Arizona State University	Grad
Matthew Snow	Radiochemistry	Washington State University	Grad

## Table 2 Seminar Schedule 2010

<u>Date</u>	<u>Speaker</u>	<u>Title of Presentation</u>
June 24	Brian Powell, Clemson university	Characterization of Actinide Speciation in Natural Systems
July 1	Ken Moody, LLNL	Forensic Radiochemistry
July 8	Kim Knight, Julie Gostic, Ruth Kips, LLNL	Post- doctoral Research in Nuclear Forensics at LLNL
July 15	Sue Clark, Washington State University	Environmental Radiochemistry
July 22	Brad Esser, LLNL	Isotope Hydrology
Aug 5	Jay Davis, former director of DTRA	Preparing for the Experiment one Hopes Never to do
Aug 12	Poster Session	



# Gamma-ray Intensity Ratio Determination of $^{235}\text{U}$

Megan E. Bennett, Nuclear Forensics Internship Program

Dawn A. Shaughnessy, Roger A. Henderson, Ken J. Moody, CSD, PLS



Glenn T. Seaborg Institute

## Background

A requirement of nuclear forensics, environmental radiochemistry, nuclear physics and the nuclear power industry is the need for quantitative identification of  $^{235}\text{U}$ . One method used to achieve this is gamma spectroscopy. To date, the energy and intensity ratio values for  $^{235}\text{U}$   $\gamma$ -ray energies above 300keV are inconsistent. The cause of this inconsistency is most likely due to summing effects in the detector. It is the goal of this study to resolve this issue and report the true intensity ratios for  $^{235}\text{U}$ .

## Method

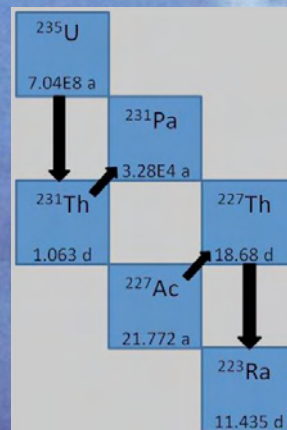
A  $^{235}\text{U}$  source on Al was made using a self-deposition technique. A self-deposited source of  $^{235}\text{U}$  was made on Al from an ~60mM  $^{235}\text{U}$  solution at pH3. The source was then transported to the nuclear counting facility at LLNL, where all measurements were made on a 30% High Purity Germanium (HPGe) spectrometer. The sample was counted at various distance and for various count times. The count times were chosen such that an adequate number of counts under the peaks of interest resulted. Each spectrum then underwent data analysis, as described below.

## Analysis

The raw data was processed with GAMANAL. The peak area in the peaks of interest were then divided by the peak area of the 185.7keV peak. This data was then plotted as a function of peak energy. The error was based on counting statistics and calculated using standard error propagation methods. The error in peak energy was smaller than the data symbol. In order to determine if a peak would be observed, a ratio of a strong, known peak and the peak of interest was taken. Detector efficiency, the given distance and emission probability were taken into account.

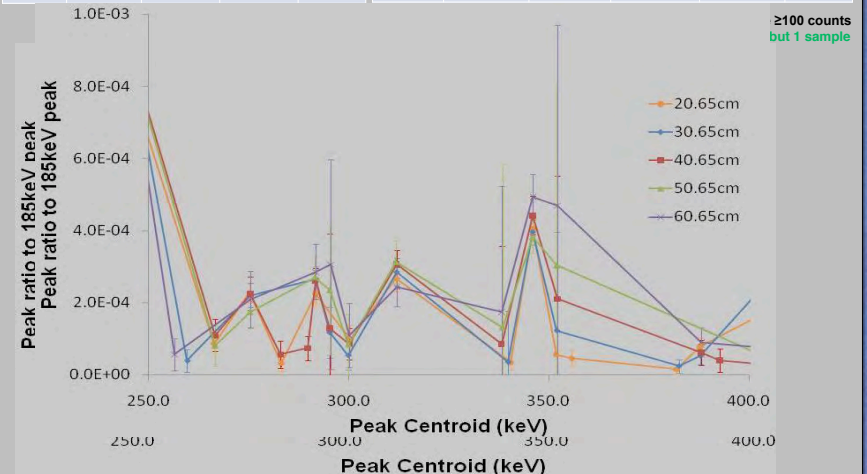
## Acknowledgements

The authors would like to acknowledge Todd Woody and Cindy Conrado of the nuclear counting facility at LLNL.



## Results

$^{235}\text{U}$ Peaks Matching TOI Reported Peaks					Remaining TOI Reported Peaks					
72.6	140.8	182.5	205.4	241.0	251.5	282.92	301.741	345.4	390.3	517.2
74.8	142.8	185.8	215.3	246.9	266.45	289.56	310.69	356.03	410.29	742.2
95.8	143.8	195.0	221.5	275.4	275.129	291.2	317.062	368.5	433.0	794.7
98.3	150.9	199.0	228.8	346.0	279.50	291.65	325.8	371.8	448.40	
109.1	163.4	202.2	233.5		281.441	294.3	343.5	387.82	455.41	



\* This is based on reported %lg in the Table of the Isotopes and calculated detector efficiency at a given energy and distance

## Conclusions

In the  $\gamma$ -ray spectrum of  $^{235}\text{U}$  24 lines reported in the Table of the Isotopes (TOI) have been confirmed, while 28 other peaks, above 200keV, reported by TOI remained unobserved. Of these 28 peaks, 11 peaks should have been observed over the duration of the data collection based on the reported intensity values in TOI. The data presented here indicates a serious discrepancy in not only the energy lines reported in TOI but also the intensity values. Determination of intensity values of the peaks seen in this is underway.





# Antineutrino Flux Calculation for a CANDU Startup



Glenn T. Seaborg Institute

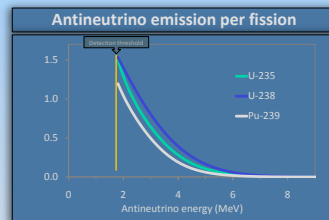
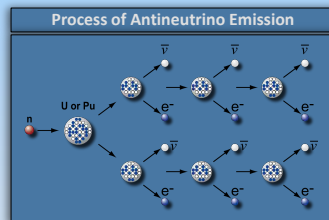
Topher Matthews, Nuclear Forensics Internship  
Adam Bernstein, Physics Division, PLS



*The antineutrino flux emitted from reactors can provide a means of external safeguards monitoring. A computer model was created to simulate the initial 100 full power days of a CANDU reactor prior to online refueling. These simulations will complement a detector to be deployed at the recently refurbished Point Lepreau CANDU reactor. Using a time dependent power map the SCALE lattice code was utilized to calculate isotopic fission rates and depletion of the fuel. The total antineutrino rate can be shown to decrease linearly after the initial startup as burnup of the fuel increases.*

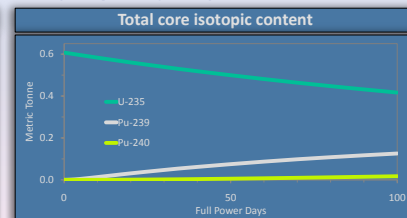
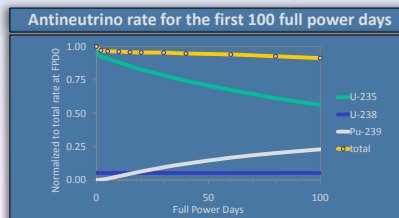
## 1) Introduction:

- Roughly six antineutrinos per fission are emitted during beta decay of fission products and their daughters. The slight difference in antineutrino spectrum between fissionable isotopes causes a changing total antineutrino rate as the fuel is depleted. The time evolution of the antineutrino rate can determine if the reactor is on or off, calculate thermal power of the core, and predict isotopic content.
- The Point Lepreau Generating Station (PLGS) CANDU-6 reactor is undergoing a complete replacement of pressure tubes to extend the lifetime of the plant. The reactor will restart with a nearly fresh core, an event that only occurs twice in CANDU's lifetime. The detector to be deployed at PLGS will measure the antineutrino rate during the transition from a startup core (no refueling, fresh fuel, decreasing fission rate) to equilibrium core (online refueling, fresh and depleted fuel, constant fission rate).
- The simulation presented here aims to predict the antineutrino rate in the first 100 days, prior to the start of online refueling.



## 3) Results:

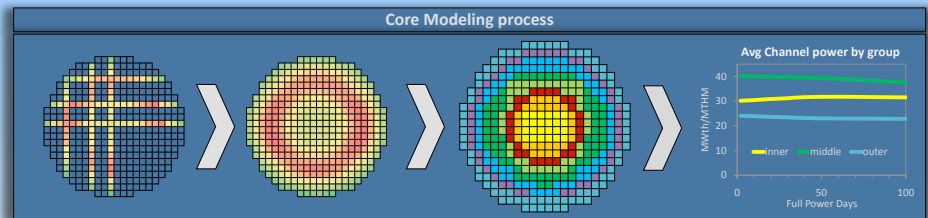
After an initial drop that may be an artifact from the simulation code, the total antineutrino rate decreases linearly. As the U-235 content decreases and Pu-239 content increases, the antineutrino rate drops due to the 25% difference in detectable antineutrino emissions between the two isotopes. The antineutrino rate closely follows the core isotopic content. The Pu-240 content reaches 7% of total plutonium content (weapons grade) on FPD 50.



## 2) Methods:

The CANDU core is made up of 380 individual pressure tubes each with 12 half meter naturally enriched fuel bundles. For the simulation, each pressure tube is modeled as a single assembly and assigned the average bundle power in that channel. A full core channel average power map was interpolated from a small data set produced by the reactor operator's safety simulations. The total core was blocked into eight regions of similar power and flux, and interpolated over 100 days.

The power data was used as input into the TRITON module in the SCALE lattice cell code to determine flux and fuel depletion using the 44-group ENDF/B-V library. Combined with microscopic cross section data, the fission rate and antineutrino rate was calculated for each isotope.



## 4) Discussion

This model shows how the antineutrino rate is highly dependent on core composition. While it does not take into account online refueling, it is still applicable until full power day 70-80.

The lower content of Pu-240 present in the fuel before full power day 50 is more desirable for nuclear weapons. A potential proliferator might replace several or all fuel channels with fresh fuel and extract the plutonium from the irradiated bundles before the percentage of Pu-240 increases to levels requiring more sophisticated separation techniques. Since the antineutrino production is closely correlated to the fuel isotopic composition, a jump in antineutrino counts could indicate early replacement of fuel bundles. More simulations need to be performed to predict the ability to detect this and several other diversion scenarios.



Glenn T. Seaborg Institute

# Neptunium Sorption to Goethite

Mathew Snow, Nuclear Forensics Internship Program

Pihong Zhao, Mavrik Zavarin, and Annie Kersting, Chemical Sciences Division, PLS



## Introduction

Large quantities of neptunium have been released into the environment as a result of nuclear weapons programs and reactor discharge.<sup>1</sup> With a half life on the order of two million years, coupled with its in-growth from parent nuclide Am-241, Np-237 also represents a major contributors to the long term (~100,000+ yrs) dose of proposed geological repositories.<sup>2</sup>

Iron oxides, such as goethite (FeOOH), are commonly found in rocks and soils. While the degree to which these minerals (ad)sorb radionuclides has wide implications on their ability to retard actinide migration, strong sorption also has the potential to increase actinide mobility via colloid-facilitated transport.<sup>3</sup> Thus, an increased understanding of neptunium-goethite interactions is essential for reliable transport models, as well as possible methods for remediation and retardation.

## Background

While Np(IV) and Np(VI) have been observed in highly reductive and oxic environments, respectively, Np(V) is the predominant oxidation state under typical environmental conditions.<sup>4</sup> Most laboratory studies have analyzed neptunium at much higher concentrations ( $>10^{-6}$  M) than are frequently observed in the environment ( $10^{-12}$  M Np observed at the Nevada Test Site), making the assumption that the processes observed in the laboratory are simply scalable to environmentally relevant concentrations.<sup>5,6,7</sup>

While neptunium-237 is the predominant neptunium isotope found in the environment, its relatively low specific activity makes it difficult to detect at lower concentrations ( $<10^{-7}$  M) using nuclear counting techniques. Thus, for this study a mixed approach was adopted, using Np-239 (half life of 2.345 days) for lower concentrations ( $10^{-18}$  to  $10^{-15}$  M), a 239/237 mixture, in which Np-239 is used as a tracer, for medium range concentrations ( $10^{-14}$  to  $10^{-9}$  M), and pure Np-237 for analysis of higher concentrations ( $10^{-8}$  to  $10^{-2}$  M).

## Objectives

- Study the Np-goethite sorption isotherm over a wide concentration range ( $10^{-18}$  to  $10^{-2}$  M)
- Analyze K<sub>d</sub> (equilibrium constant) as a function of aqueous concentration
- Implement novel approach using short lived Np-239 tracers to extend the sorption isotherm to concentrations that are comparable to or lower than Np concentrations observed in the environment

## Methods

### Np-239 Purification

- Milked from Am-243
- 1 mL 50-100 mesh AG BioRad column
- 50:1 HCl:H<sub>2</sub>O load solution
- Am-243 collected in the effluent, purified Np-239 eluted using 1M HCl + 0.05M HF

### Np-237 Purification

- Purification from Pa-233 daughter
- 2 mL 100-200 mesh AG BioRad column, concentrated HCl load solution
- Pa-233 eluted using 9M HCl + 0.05 M HF
- Np-237 eluted using 6M HCl + 0.05 M HF
- Repeated procedure until >99% pure solutions obtained (determined by LSC alpha/beta discrimination and gamma counting)

Low Concentrations  
( $10^{-18}$  to  $10^{-15}$  M)

Mid-Range Concentrations  
( $10^{-14}$  to  $10^{-9}$  M)

High Concentrations  
( $10^{-8}$  to  $10^{-2}$  M)

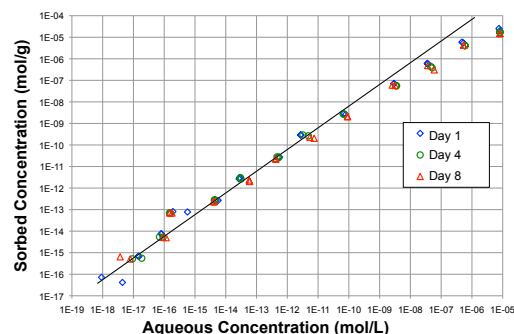
### Np(V) Characterization

- Solutions reconstituted in 5M HNO<sub>3</sub> to fix the Np oxidation state at (V) and (VI)
- Np was oxidized to (VI) in concentrated HNO<sub>3</sub> then reduced to (V) in 5M HNO<sub>3</sub> using H<sub>2</sub>O<sub>2</sub>
- Oxidation state was verified using UV-Vis for Np-237 stock solutions. UTEVA column was used to confirm Np(V) for Np-239 spike solutions.

### Sorption Study

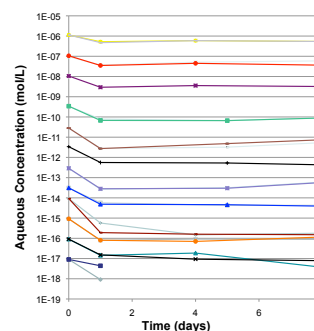
- 18.8 m<sup>2</sup>/g goethite prepared using established procedure<sup>8</sup>
- Goethite suspended in a solution of 5mM NaCl + 0.7mM NaHCO<sub>3</sub> with 18Ω MQ H<sub>2</sub>O
- pH maintained at pH 8.0 ± 0.5
- Solutions constantly mixed using rotary mixer
- Sampling performed approximately 1, 4, and 8 days after Np addition
- Samples were centrifuged at 3000 RPM for 2hrs to ensure adequate solid-liquid separation
- Np-239 and/or Np-237 in the supernatants were analyzed using LSC, with selected sample verifications using gamma counting and ICP-MS

## Results



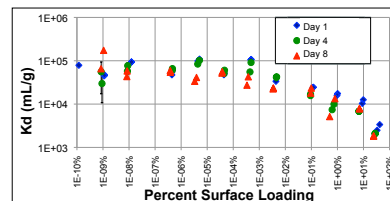
Sorption curve for Neptunium to goethite

- Sampling performed on days 1, 4, and 8 after addition of neptunium (represented in blue, green, and red respectively)
- Data follows a linear trend for neptunium concentrations between  $10^{-18}$  to  $10^{-10}$  M
- Begins to deviate from linearity at concentrations higher than  $10^{-10}$  M
- Approaches surface saturation at  $\sim 10^{-2}$  M.



Rate Dependence of Sorption

- Equilibrium reached within first day
- Spiked blank samples showed ~15% activity loss due to sorption on container walls
- Minor increases in concentration in certain samples as a result of changes in pH

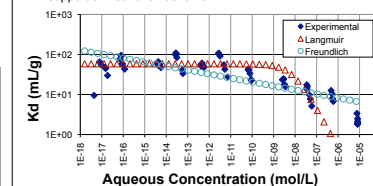


K<sub>d</sub> as a function of percent surface loading

- K<sub>d</sub> relatively constant from  $10^{-10}$  to  $10^{-4}$ % site occupation
- Decreases exponentially at concentrations greater than  $10^{-4}$ %

### Preliminary Sorption Modeling

- Concentrations  $<10^{-10}$  M aqueous Np ( $<10^{-4}$ % site occupation) support a Langmuir behavior
- Concentrations  $>10^{-10}$  M aqueous Np ( $>10^{-4}$ % site occupation) support a Freundlich behavior



## Conclusion

- Np-goethite sorption reaches equilibrium within 1 day
- K<sub>d</sub> relatively constant between  $10^{-18}$  and  $10^{-10}$  M ( $10^{-10}$  to  $10^{-4}$ % surface loading) then decreases exponentially from  $10^{-10}$  to  $10^{-2}$  M
- Np-239 tracers found to extend detection limits down to  $\sim 10^{-18}$  M concentrations
- Future work includes improving modeling capabilities using 2-site Langmuir and similar approaches to elicit more information on Np-goethite sorption site affinity

## References

1. Smith, D.K., Friesen, D.L., and Breen, S.M. 2003. Journal of Environmental Radioactivity 67, 35-51.
2. Turner, D.R., Bertelli, F.P., Pabalan, R.T. Soil Science Society of America: Madison, WI, 2002; pp111-252
3. Kersting, A.B., D.W. Stout, D.L. Friesen, D.J. Risop, D.K. Smith, J.L. and Thompson, (1999). Nature 397, 56-59
4. Dzozic, M., Haggmann, R. Pure Appl Chem 1992, 65, 1081-1102
5. Aral, Y., Moran, P.B., Honeyman, B.D., and Davis, J.A., 2007. Environmental Science & Technology 41, 3940-3944.
6. Nakayama, S. and Sakamoto, Y., 1991. Radiochimica Acta 52-3, 153-157.
7. Turner, D.R., Pabalan, R.T., and Bertelli, F.P., 1998. Clays and Clay Minerals 46, 256-269.
8. Schweitzer, U. and Cornell, R.M. 1991. VCH Publishers Inc., New York, NY.



Glenn T. Seaborg Institute

## Design of a Compton Vetoed Ge Detector For Direct Measurement of Pu in Spent Nuclear Fuel

Cameron Bates, Nuclear Forensics Internship Program

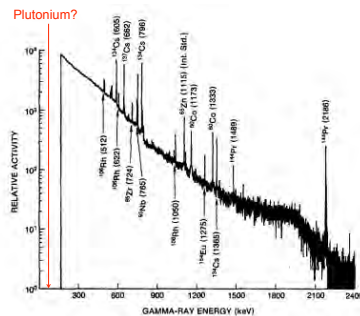
Stephan Friedrich, Physics - Physical and Life Sciences



### Motivation: Where is the plutonium?

A typical 1-GWe power plant discharges up to 30,000 kg of spent fuel per year. Of that roughly 300 kg is Pu. Even though it is a small amount of the total mass of spent fuel it is enough for 30 nuclear devices (~10 kg per device). This becomes an issue when the fuel is reprocessed, because the Pu is separated from highly radioactive fission products. If it is not possible to determine how much Pu was in the fuel prior to dissolution, there is no way to verify that none was diverted.

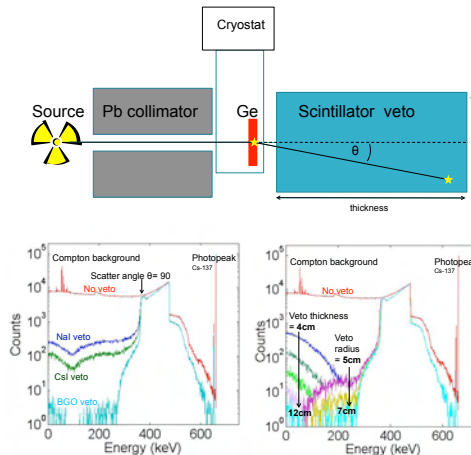
### Direct Pu measurement is currently impossible



Spent fuel spectrum<sup>1</sup>: Pu is masked by Compton scattering from Cs and other fission products

### Approach: *Thin* HPGe detector with a Compton veto *behind* it

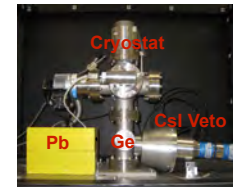
- Veto rejects low angle Compton scatter into region of interest
- HPGe has the energy resolution to resolve low energy Pu X-rays
- Ge and scintillator geometry optimized to improve veto
- Cs-137 used for system characterization
- Scintillator material chosen to optimize rejection



Scintillator material choice: maximize stopping power

Optimization of scintillator geometry: as large as possible

### Results: Prototype setup

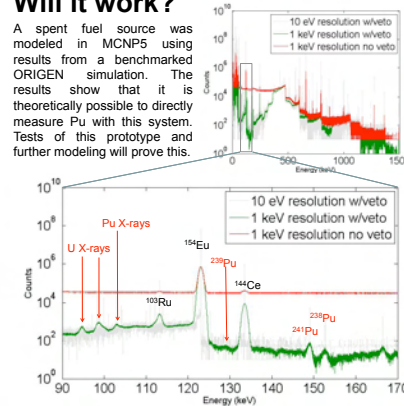


- 30x30x8mm<sup>3</sup> planar Ge detector
- 8" Pb collimator
- 2xCsI veto:
  - 3"Øx6"
  - 6"Ø(outer)x3"
- Pulse tube cooler

### Will it work?

A spent fuel source was modeled in MCNP5 using results from a benchmarked ORIGEN simulation. The results show that it is theoretically possible to directly measure Pu with this system. Tests of this prototype and further modeling will prove this.

Simulated spent fuel spectra



References: 1. Passive Nondestructive Assay of Nuclear Materials. Office of Nuclear Regulatory Research, 1991.



Glenn T. Seaborg Institute

# <sup>35</sup>S: New Tracer of Groundwater Travel Time Near MAR Operations

Stephanie Diaz, Nuclear Forensics Internship Program  
Bradley Esser, Richard Bibby, Chemical Sciences Division, PLS



## Introduction

- Managed artificial recharge (MAR) is a water management tool designed to augment water supplies.
- Current CA regulation requires the location of municipal wells to be 150 m from MAR unless a six month travel time can be determined.
- Dating MAR water has previously involved extensive field work (gas tracers: SF<sub>6</sub>, Xe) or utilizing isotopes with longer lived half lives.
- <sup>35</sup>S is a cosmogenically produced radionuclide (t<sub>1/2</sub>=87 days) that has been useful for studying recharge in alpine basins, but its application in MAR studies has been limited due to high SO<sub>4</sub> concentrations.

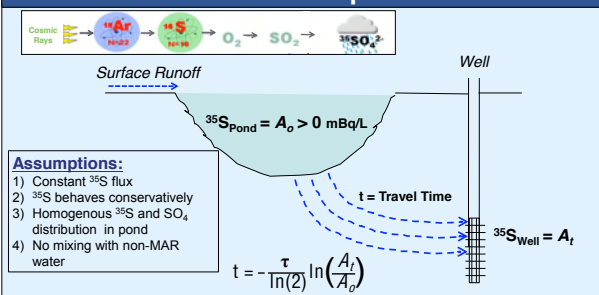
### Project Goals:

- 1) Refine method for natural waters containing high SO<sub>4</sub>
- 2) Evaluate potential of <sup>35</sup>S method to estimate groundwater travel times at two MAR locations: Rio Hondo Spreading Grounds (RHSG) and Alameda County Water District (ACWD) (Fig 1)



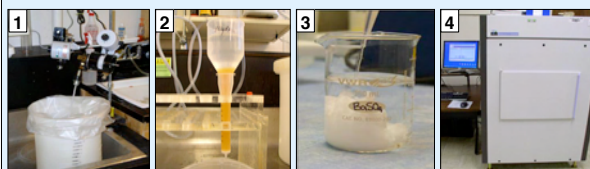
Figure 1. Location of MAR study sites and RHSG recharge pond.

## Model of MAR Operations



## Analytical Methods

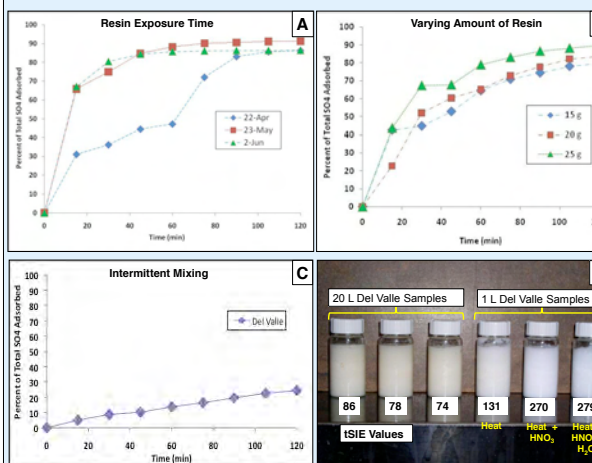
Samples collected and processed based on modified techniques from Michel et al., (2000):



- 1) Process approximately 1000 mg SO<sub>4</sub> per sample by acidifying and suspending Amberlite ion exchange resin in sample for 2 hrs
- 2) Elute SO<sub>4</sub> from resin with NaCl solution
- 3) Add BaCl<sub>2</sub> to precipitate BaSO<sub>4</sub>
- 4) Suspend BaSO<sub>4</sub> in Instagel for liquid scintillation counting

### Method Development for Natural Waters

To refine the method for higher SO<sub>4</sub> MAR waters, the following variables were examined: pH effect on SO<sub>4</sub> adsorption, sample exposure time to resin (Fig A), total amount of resin (Fig B), intermittent mixing of resin in sample (Fig C), and effects of heat, HNO<sub>3</sub>, H<sub>2</sub>O<sub>2</sub> on color quenching (Fig D).



## Results

### Method Refinement

- Varying the pH (pH 1 to pH 7) and total amount of resin (15 g to 25 g) had little effect on SO<sub>4</sub> adsorption
- Continued mixing of resin in sample was more effective in adsorbing SO<sub>4</sub> relative to intermittent mixing.
- Exposing the BaSO<sub>4</sub> precipitate to heat and HNO<sub>3</sub>, or HNO<sub>3</sub> and H<sub>2</sub>O<sub>2</sub> resulted in a higher tSIE values, suggesting that these treatments reduce the quench associated with a sample.

### Travel Time Estimates

Table 1. Comparison of travel time determined by <sup>35</sup>S to previous tracer studies.

Well	Date Collected	SO <sub>4</sub> (mg/L)	<sup>35</sup> S (mBq/L)	<sup>35</sup> S Travel Time (days)	Tracer Travel Time (days)	Tracer
RHSG-Pond	2 June 2010	184.0	8.76	NA	NA	NA
RHSG-MW1	22 Apr 2010	105.7	3.60	75	46	SF <sub>6</sub> *
RHSG-MW1	23 May 2010	146.0	2.89	89	46	SF <sub>6</sub> *
ACWD-B Pond	14 Jul 2010	86.5	2.76	NA	NA	NA
ACWD-B	14 Jul 2010	79.9	0.04	MDA	56	<sup>124</sup> Xe**
ACWD-K Pond	14 Jul 2010	90.7	3.86	NA	NA	NA
ACWD-K	14 Jul 2010	93.3	0.74	173-235	<20	<sup>136</sup> Xe**

\*McDermott et al. (2008) \*\*Moran and Halliwell (2003)

## Conclusions

With the exception of one monitoring well in ACWD, <sup>35</sup>S activity in the ponds and wells was above MDA. As expected based on the simplified model, <sup>35</sup>S activity was higher in MAR surface water from the ponds relative to the groundwater from the wells. The older travel times resulting from the <sup>35</sup>S method relative to previous studies may be due to mixing or water-rock interactions that are not accounted for by this simplified model. These preliminary results demonstrate the potential use of <sup>35</sup>S as a tracer in MAR operations.

### Future Studies

- Further comparison of age dated MAR wells with varying travel times using <sup>35</sup>S method
- Determine seasonality of <sup>35</sup>S activity in MAR surface and groundwater
- Determine potential stratification of <sup>35</sup>S and SO<sub>4</sub> within MAR ponds

### Acknowledgements

This work was completed with the help of J. Moran, S. Roberts, M. Holtz, E. Dieck from LLNL, and B. Chong from the Water Replenishment District of Southern California.

### References

Moran, J., and M.S. Halliwell, 2003. Characterizing Groundwater Recharge: A Comprehensive Isotopic Approach. *Awara Research Foundation*.  
McDermott, J., D. Avissar, T.A. Johnson, and J.F. Clark, 2008. *J. Hydrologic Engng.* 13: 1021-1028.  
Michel, R.L., D. Campbell, D. Clow, and J.T. Turk, 2000. *Water Resour. Res.* 36: 27-36.





# Uranium and Plutonium Isotope Detection Using Coincidence Methods



Glenn T. Seaborg Institute

Steven Horne, Nuclear Forensics Internship Program, University of Texas  
Dr. Tzu-Fang Wang, Chemical Sciences Division, PLS, Lawrence Livermore National Lab

## ABSTRACT

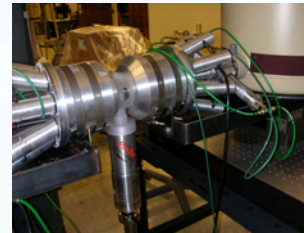
In this project, we aim to look at uranium and plutonium samples using coincidence counting methods. The main isotopes of interest were uranium-235, uranium-238, plutonium-239, and plutonium-240. As a result of this project, we were able to determine the isotopic ratios for our premade samples using coincidence techniques, which could play a key role in nuclear non-proliferation and accountability.

## INTRODUCTION

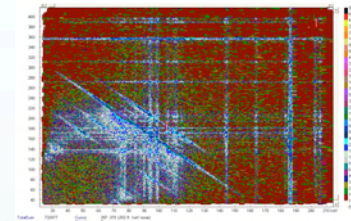
- Can we take a uranium or plutonium sample and figure out its isotopic ratios with a high amount of background present?
- High resolution gamma ray spectrometry has been in use for over 50 years and is useful for element and isotope detection in environmental, biological, and radioactive samples.
- Using multiple detectors, one has the capability of looking at isotopes with cascading decays without interference from the Compton continuum of fission products with high energy gamma rays.
- Using these techniques, we can determine uranium or plutonium isotope ratios, even in the presence of fission products.

## METHODS

We used a total of three high purity germanium detectors. The two coaxial detectors are useful for looking at gamma rays of high energy (100 – 1800 keV), and the planar detector is useful for looking at gamma rays of low energy (20 – 300 keV). Using a list mode data acquisition system we are able to detect gamma-rays from the samples with a coaxial – coaxial coincidence and a coaxial – planar coincidence configurations. By analyzing energies and time of the data among the detectors, we are able to determine the isotopic ratios using the ratios of the energy gated coincidence events. We verified this technique using three known isotopic compositions of uranium gamma-ray standards consisting of .5%, 5%, and 50% U-235.

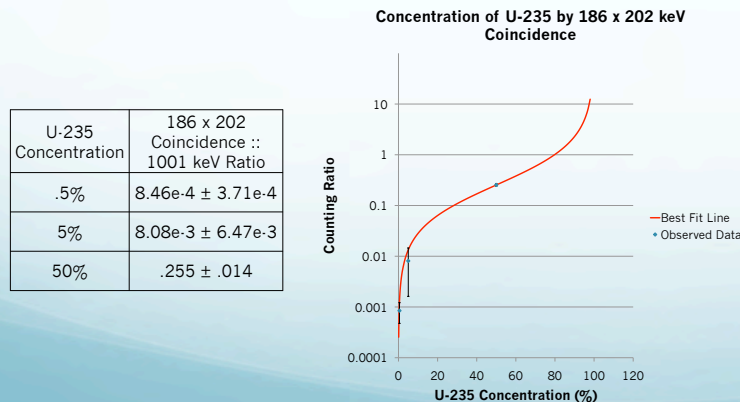


The above figure shows the three detectors in use – on the left and right are the two coaxial detectors, and on the bottom is the planar detector.



The above graph is an example of a coaxial - coaxial coincidence spectrum being analyzed. Red and green spots correspond to a lower number, while the blue and white spots correspond to more coincidences. The axes correspond to the channels of the respective detectors. This spectrum came from the 50% U-235 sample.

## RESULTS



## DISCUSSION

When attempting to determine the concentration of U-235 in a sample, one often looks at the 186 keV peak in the spectrum. This peak is often interfered with by the Compton continuum produced by long-lived fission products. In order to overcome this barrier, we utilize the coincidence counting method, with which we compare the ratios of the 186 – 202 keV coincidence peaks to the 1001 keV single peak, which is of high enough energy to not be affected by the Compton continuum. From this method, we can develop an equation to predict the concentration of U-235 in an unknown sample. With the results achieved, we can estimate the equation of best fit to be  $y = x / (.254 + x)$ , where  $x$  is the ratio of 186 x 202 keV coincidences to 1001 keV single counts and  $y$  is the concentration of U-235 in the sample. This estimation does take into consideration the dead time of the counts. In order to fully demonstrate the effectiveness of the method, we need to look at the angular dependence of the cascading emissions, as well as the efficiencies of the detectors in use.





Glenn T. Seaborg Institute

# Separation and isotopic analysis of activation products for nuclear forensics

Meghali Chopra, Nuclear Forensics Internship Program

Aaron Glimme, Department of Energy Academies Creating Teacher Scientists

Scott Tumey, Atmospheric, Earth and Energy Division, PLS

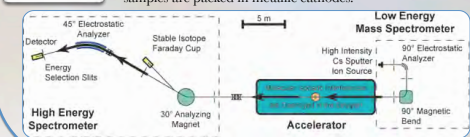
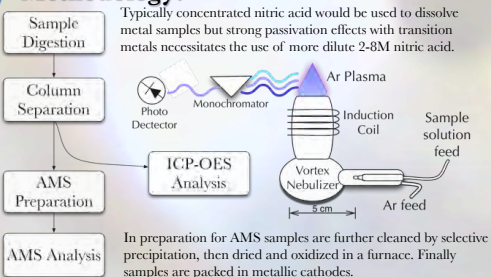


**Abstract:** We separated and prepared various metal samples for isotopic characterization by accelerator mass spectrometry (AMS) including aluminum, iron, nickel and cobalt. Separations were performed using column chromatography and selective precipitation. Initial concentration measurements were performed using inductively coupled plasma optical emission spectroscopy (ICP-OES) and the performance of various AMS cathode matrix metals was evaluated with high purity iron samples.

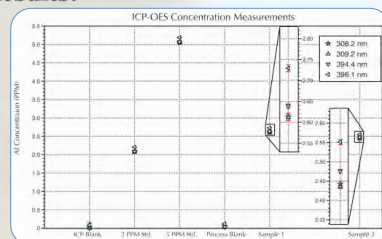
## Introduction:

Nuclear forensics plays a crucial role in the deterrence of nuclear terrorism. Transition metal activation products can provide valuable information about the components and method of delivery of a nuclear device. Unfortunately the prevalence of large background quantities of metals such as aluminum, iron, nickel, and cobalt mean that the activation products of transition metals must be measured against a large background signal. Isotopes of iron, cobalt and nickel have stable isobars that can make measurements particularly difficult. Two possible approaches to these problems are improved detector discrimination and the use of chemical differences to separate the isobars before analysis. Our focus has been on chemical differences that will allow the determination of transition metal isotope ratios with unparalleled accuracy in this challenging sample environment.

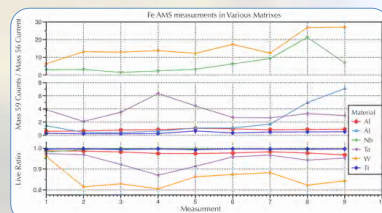
## Methodology:



## Results:



The concentrations of known standard solutions were first measured using ICP-OES. After a linear calibration curve had been established, the three unknowns were measured. Based on the initial calibration, sample 1 had a concentration of  $2.613 \pm 0.008$  ppm, sample 2 had a concentration of  $2.439 \pm 0.005$  ppm, and the process blank had a concentration of  $0.0477 \pm 0.005$  ppm.

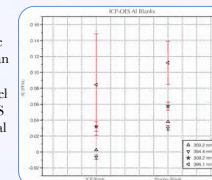


Iron samples were analyzed by AMS to determine the effects of different cathode materials. High purity iron samples were loaded into cast aluminum and pressed powder matrices of niobium, tantalum, tungsten, and titanium. These samples were run on the AMS tuned to count mass 59 and measure the current of mass 56 isotopes.

## Discussion:

A key component to achieving accurate AMS isotopic measurements is the minimization of unwanted isobars. For sample preparation, this means chemically separating the elements of interest from those that interfere with the AMS measurements. This is particularly difficult with iron, cobalt and nickel because they have very similar chemical properties. Typical separations developed for geological applications are time consuming. Rapid analysis is a critical requirement for forensics, so our focus has been aimed at developing less time-intensive separation methods.

Our initial results indicate the most commonly used cathode materials are all well suited to use with iron AMS analysis. Outliers in the data can be attributed to a skewed normalization as the live ratio begins to drop. Tests for optimal nickel and cobalt matrices are also ongoing. ICP-OES results for aluminum were consistent with initial estimates based on the size of the aluminum samples originally digested.



One item of note is the slightly elevated concentration of the digestion process blank. More analysis of the materials and process used in the initial digestion is needed to ensure that no additional aluminum is being inadvertently added during the digestion. Efforts to accurately detect iron, cobalt, and nickel via ICP are ongoing and will constitute a vital factor in ensuring the completeness of the chemical separation.

## Implications:

Additional work remains for the development of a complete separation and analysis protocol. First, more analysis of the purity that can be achieved by our combination of column and precipitation separation is needed. Future experiments will include ICP measurements of iron, cobalt, and nickel solutions as well as AMS measurements of cobalt and nickel in their aluminum, niobium, tantalum, tungsten and titanium matrices. Second, the new AMS detector designed for the separation of iron, cobalt, and nickel isobars must be validated. After the sample preparation process has been refined and the AMS detector has been optimized, it will be possible to very quickly characterize the activation products for iron, cobalt and nickel from real world backgrounds with unprecedented sensitivity.



# Geolocation of Nuclear Materials



Greg Brenneka - Nuclear Forensics Internship Program

Lars Borg - Chemical Science Division, PLS

Uranium ore concentrate (UOC), or “yellowcake”, is the final product in the mining and milling of uranium ore, and represents an intermediate step in the utilization of uranium for its energy potential.

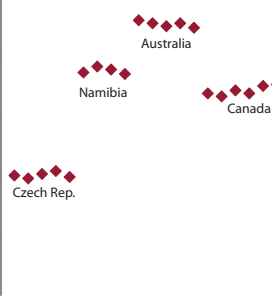
Yellowcake is a fungible commodity that is commonly traded worldwide, but is also a regulated nuclear material. In cases of illicit trafficking, chemical impurities and isotopic signatures imparted on the UOC by the source rock and/or mining process have the potential to allow the UOC to be traced to its point of origin. High precision isotopic ratios from a few key elements can provide invaluable clues to the provenance of illicit material.



Sr Nd

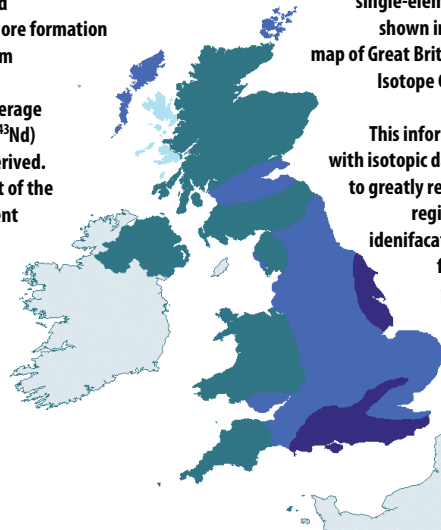
The Strontium (Sr) and Neodymium (Nd) isotopic composition of uranium ore is dictated by 1) the composition inherited at the time of ore formation and 2) radiogenic ingrowth from  $^{87}\text{Rb}$  and  $^{147}\text{Sm}$  parent isotopes. Thus, Sr and Nd isotopic compositions of UOC represent a long-term average parent/daughter ratio (i.e.,  $^{87}\text{Rb}/^{87}\text{Sr}$ ;  $^{147}\text{Sm}/^{143}\text{Nd}$ ) of the rocks in the region from which UOC is derived. Chemical separation of Sr and Nd from the rest of the elements in UOC to enable precise measurement of isotopic ratios for each element for use in geolocation.

$^{87}\text{Sr}/^{86}\text{Sr}$

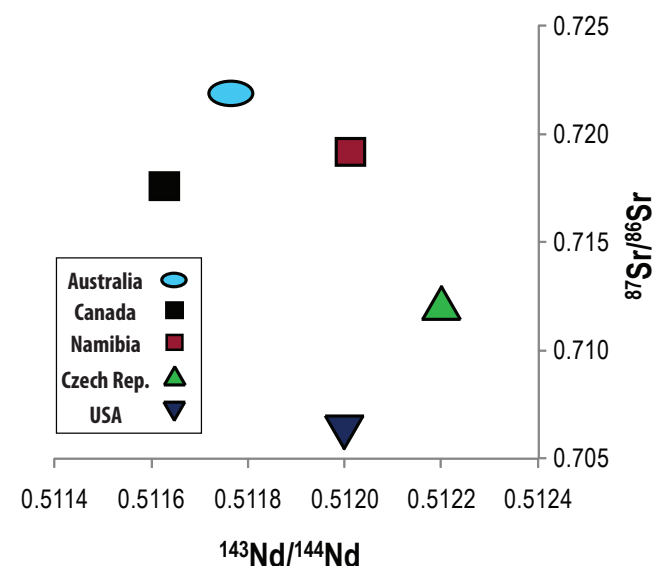
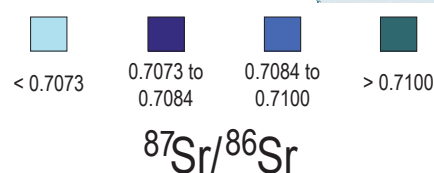


Sr isotopes values from UOC are shown, representing a few of the hundreds of UOC producing regions from around the world. Knowledge of only one isotope ratio does not produce unique values for each region, but can greatly narrow the search.

The isotopic data obtained from UOC can be used to produce single-element maps of a region, as shown in this bedrock Sr isotope map of Great Britain (redrawn from NERC Isotope Geosciences Laboratory).



This information can be combined with isotopic data from other elements to greatly reduce the possible source regions of UOC. This permits identification of a unique isotopic fingerprint for many UOC producing regions of the world. An example of this is shown using Sr and Nd isotopic values, illustrating five unique signatures.



Determining of the provenance of a sample of UOC requires a variety of techniques and methods. Certain isotopic systems, such as Sr and Nd, have proven to be particularly useful in determining the type of rock from which nuclear material was derived, a critical step in the geolocation of a sample of unknown origin.



## Determination of uranium ore concentrate source using multivariate signatures: assessing single-sample models with ROC curves

Glenn T. Seaborg Institute

Marianna Mao, Nuclear Forensics Internship Program  
Martin Robel, Chemical Sciences Division, PLS



Nuclear forensic analysis can help determine the provenance of interdicted or declared nuclear material by identifying material characteristics (signatures) particular to its geographic or processing origins. Regression models (classifiers) calibrated on an existing database of known materials extract the comparative multivariate signatures that most differ from one source (class) to another. Based on these signatures, unknown samples are then assigned to a class in the database with some degree of confidence. Normally, signatures are inferred from classifiers trained on multiple samples per class. However, in the case of nuclear material, often only one sample per class can be obtained. I assess the performance of such single-sample models.

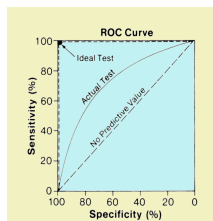
### Introduction

For nuclear safeguards, non-proliferation, or law-enforcement applications, nuclear forensic analysis may be used to determine or verify the declared origins of uranium ore concentrate (UOC). Multivariate signature analysis (e.g., trace element concentrations) can be used to help determine the origins of a given UOC sample through comparison of the unknown sample to a database of known samples. However, since the database contains only one sample per class for some classes, models built on this database are weakened by the lack of information on in-class scatter. In this project, I characterize the performance of models calibrated on single samples.



UOC (yellowcake) sample.

### Methods

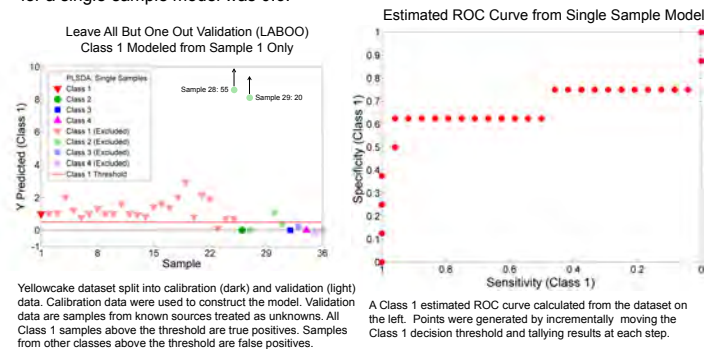


A classifier's performance depends on both its sensitivity (the number of true positives correctly identified) and specificity (the number of true negatives correctly identified). As the decision boundary is made stricter, the sensitivity of the classifier decreases while the specificity increases. This relationship is illustrated by the ROC curve, which plots sensitivity and specificity as the boundary is changed. The area under the ROC curve can be used to compare different models and to gauge confidence interval outputs.

ROC curves cannot be calculated for a model based on single-sample data because in-class variance can only be inferred from a distribution of samples. Hence, we split a dataset with multiple samples per class into a single-sample calibration set and a validation set and manually calculated estimated ROC curves based on the validation data.

### Results

The ROC area was calculated by varying the decision boundary based on the y-predicted intervals from the validation data. After obtaining a discrete number of points on the ROC curve, the area was computed by the trapezoid method. The average area for a single-sample model was 0.6.



Yellowcake dataset split into calibration (dark) and validation (light) data. Calibration data were used to construct the model. Validation data are samples from known sources treated as unknowns. All Class 1 samples above the threshold are true positives. Samples from other classes above the threshold are false positives.

A Class 1 estimated ROC curve calculated from the dataset on the left. Points were generated by incrementally moving the Class 1 decision threshold and tallying results at each step.

### Conclusion

Although the single-sample model's area of 0.6 was low compared to the near-1 areas of models with multiple samples per class, the limited amount of data made for a conservative estimate of the area, while the calculation for the model with multiple samples is a relatively optimistic one. Overall, the calculation shows that models based on single samples are still viable tools for nuclear forensic analysis.



# Development and Characterization of $^{10}\text{B}$ Containing Thermal Neutron Capturing Materials

J. Oiler<sup>1</sup>, Nuclear Forensics Internship Program

L.F. Voss<sup>2</sup>, A.M. Conway<sup>2</sup>, Q. Shao<sup>2</sup>, C.E. Reinhardt<sup>2</sup>, R.T. Graff<sup>2</sup>, D.M. Estrada<sup>2</sup>, R.J. Nikolic<sup>2</sup>

1. Arizona State University; Tempe, AZ, 85287

2. Lawrence Livermore National Laboratory; Livermore, CA, 94550



Glenn T. Seaborg Institute

## ABSTRACT

Development of a solid-state thermal neutron detector is on-going at LLNL. The detector incorporates silicon pillar PIN diodes at high aspect ratios with the trenches in between the pillars filled with  $^{10}\text{B}$ . The summer project was to expand on the existing work in two important areas:

- 1) Design, build, and carryout a thermal neutron particle experiment to directly compare different boron capturing compounds
- 2) Develop a fabrication process for a detector incorporating the neutron capturing material boron oxide.

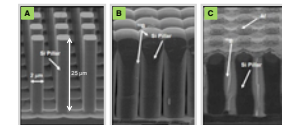
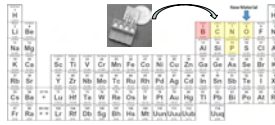
The thermal neutron experiment has been designed, the components have been delivered and are currently being set up and tested. A basic fabrication process for the boron oxide detector is completed, but optimization is still on-going.

## INTRODUCTION

Detection of thermal neutrons is important in the fields of astronomy, physics, and homeland security. Presently, thermal neutron detection is carried out using helium-3 tubes, but these devices are costly, power hungry, large in size, and not robust. Therefore, moving to the use of solid-state thermal neutron detectors is desirable. Small, portable, low power, and robust sensors would allow for easier screening of shipping containers and airport luggage for hazardous radioactive materials.

There are a number of solid-state detectors incorporating different boron compounds<sup>1-4</sup>. Each of these detectors may use a different boron compound (e.g. boron, boron carbide, boron nitride, boron phosphide). Furthermore, each of these materials may be deposited using multiple methods. These materials and depositional methods may result in different neutron sensitivities.

The solid-state thermal neutron detector researched at LLNL uses a 3-D high aspect ratio pillar structure. The silicon is doped to be a PIN diode and undergoes deep reactive ion etching (DRIE) to form pillar structures (A). Next, the gaps between the pillars are filled with  $^{10}\text{B}$  using chemical vapor deposition (B) (work done at University of Nebraska-Lincoln). After removing the excess B, Al electrodes are deposited on top and bottom of the device (C) for electronic readout.

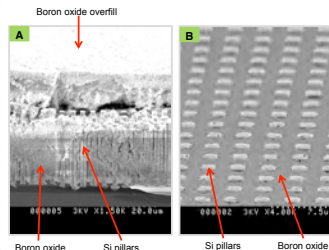


## BORON OXIDE

Elemental boron is an excellent material for solid-state thermal neutron detectors due to very high thermal neutron cross-section and its ability to be used in MEMS fabrication processes. However, we wanted to see whether isotopically enhanced boron oxide could also be used as a thermal neutron capturing material because boron oxide is a cheap material that requires non-vacuum based processing. We have had success with the initial boron oxide fabrication and process optimization is under way before device testing.

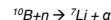
The boron oxide device fabrication process described below is the same as the boron device fabrication in steps 1, 2, 5.

- 1) Spin and pattern photoresist with pillar geometry on a wafer with a PIN Si diode structure.
- 2) Use DRIE to etch 3-D pillar geometry into substrate.
- 3) Pipette a saturated solution of enriched 10-boron oxide powder (Ceradyne Boron Products, LLC) and methanol over the entire wafer. Bake the wafer at 500 °C to allow the boron oxide to melt and flow into the etched trenches and anneal (A).
- 4) Polished back overfilled boron oxide glass using a slurry of oil and alumina particles (B).
- 5) Deposit aluminum electrodes on the top and bottom of the structure.



## BORON COMPOUND SENSITIVITY EXPERIMENT

The capture of a thermal neutron causes a  $^{10}\text{B}$  atom (thermal neutron cross-section of 3837 barns) results in an immediate decay via the following reaction<sup>5</sup>:



In 94% of reactions the Li and  $\alpha$  particles have energies of 0.84 MeV and 1.47 MeV, respectively. In the other 6%, the Li and  $\alpha$  particles have energies of 1.01 MeV and 1.78 MeV. The detector's sensitivity to thermal neutrons will be directly related to the density of the  $^{10}\text{B}$  within the thermal neutron capturing boron compound.

Directly comparing different detectors is a challenge for the following reasons:

- 1) Design and fabrication of each of these detectors may be different; they can have different size sensing areas, geometries, noise levels, amount of material, etc.
- 2) Sensitivity of a device or material in one lab may not match results in another lab with the same test setup. Because thermal neutrons will scatter off many materials and be absorbed by a host of others, neutrons scattered from all directions (not simply just in a direct line from the source) will be delivered to the detector. Therefore, the geometry, structure, and setup of the entire lab will play a role into the directional flux of thermal neutrons.
- 3) Fabricating working devices for material comparisons can be very time consuming.

For these reasons, we are constructing an experiment where we can compare different boron containing materials and boron deposition processes to one another by depositing the material on silicon, thereby eliminating issues of using different devices and saving time on device fabrication.

## Experiment setup diagram



## Alpha particle detector



## REFERENCES

- 1) Knoll, G.F., Radiation Detection and Measurement, 3rd Ed. (Wiley, New York, 2000).
- 2) Nikolic, R.J., Conway, A.M., Reinhardt, C.E., Graff, R.T., Wang, T.F., Deo, N., and Cheung, C.L., Applied Physics Letters, 93, 133502, 2008.
- 3) Osberg, K., Scherm, N., Balkir, S., Brand, J.J., Halbeck, S., Dowden, P.A., Hoffman, M.W., IEEE Sensors Journal, 6, 1531, 2006.
- 4) Uher, J., Pospisil, S., Linhart, V., Schieber, M., Applied Physics Letters, 90, 124101, 2007.

## **Disclaimer**

This document was prepared as an account of work sponsored by an agency of the United States government. Neither the United States government nor Lawrence Livermore National Security, LLC, nor any of their employees makes any warranty, expressed or implied, or assumes any legal liability or responsibility for the accuracy, completeness, or usefulness of any information, apparatus, product, or process disclosed, or represents that its use would not infringe privately owned rights. Reference herein to any specific commercial product, process, or service by trade name, trademark, manufacturer, or otherwise does not necessarily constitute or imply its endorsement, recommendation, or favoring by the United States government or Lawrence Livermore National Security, LLC. The views and opinions of authors expressed herein do not necessarily state or reflect those of the United States government or Lawrence Livermore National Security, LLC, and shall not be used for advertising or product endorsement purposes.

## **Auspices**

Lawrence Livermore National Laboratory is operated by Lawrence Livermore National Security, LLC, for the U.S. Department of Energy, National Nuclear Security Administration under Contract DE-AC52-07NA27344.